

High-throughput Mapping of Brain-wide Activity in Awake and Drug-responsive Vertebrates†

X. Lin^a, S. Wang^a, X. Yu^a, Z. Liu^c, F. Wang^c, W. T. Li^b, S. H. Cheng^b, Q. Dai^b and P. Shi^{*a,d}

^aDepartment of Mechanical and Biomedical Engineering, 83 Tat Chee Ave, City University of Hong Kong, Kowloon, Hong Kong SAR, China 999077 Email: pengshi@cityu.edu.hk

^bDepartment of Biomedical Science, 83 Tat Chee Ave, City University of Hong Kong, Kowloon, Hong Kong SAR, China 999077

^cBeijing Institute of Biotechnology, Beijing, China 100071

^dShenzhen Research Institute, City University of Hong Kong, Shenzhen, China 518057

†Electronic Supplementary Information (ESI) available.

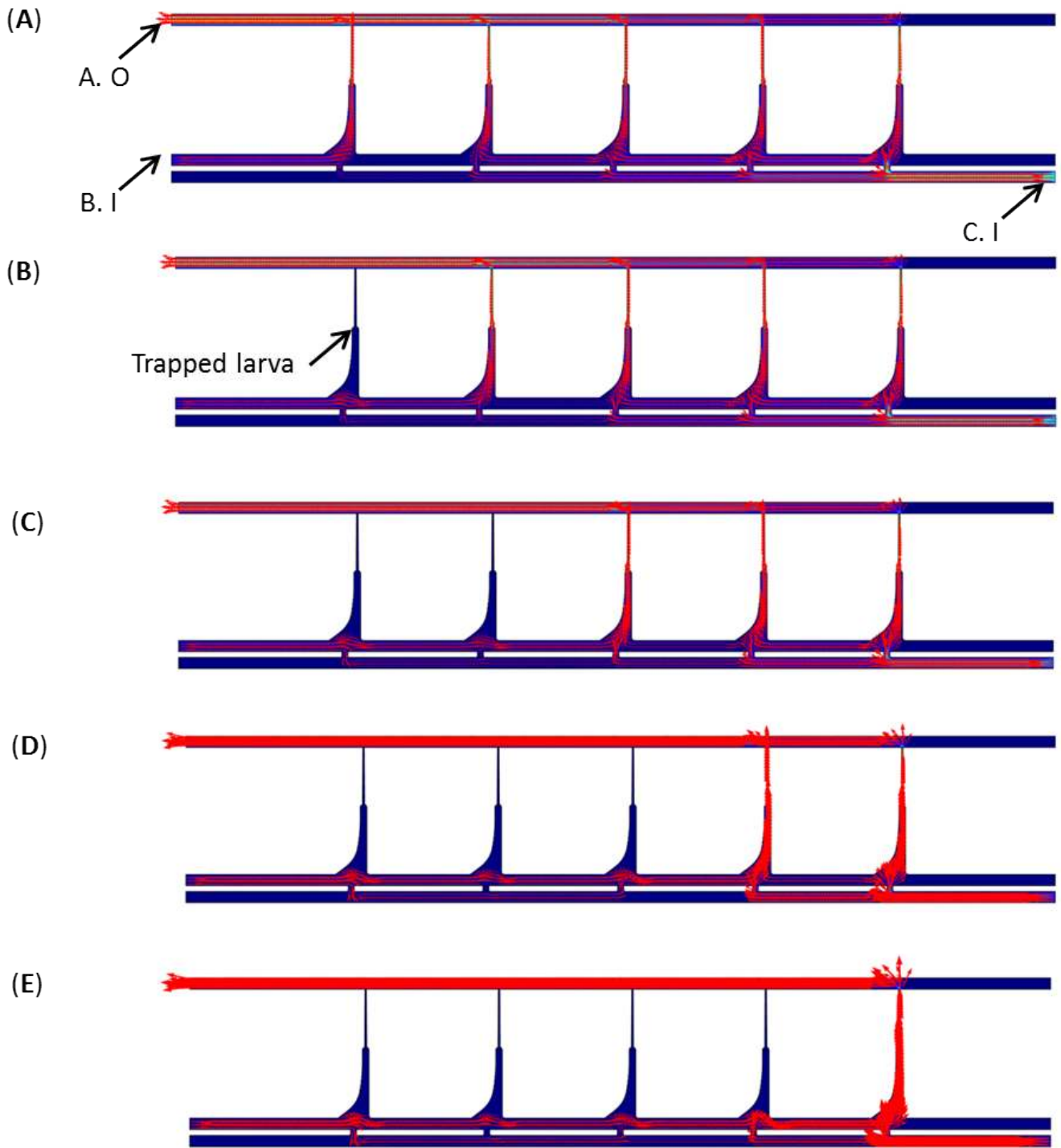


Figure S1. Simulation of the flow distribution in a Fish-Trap chip with sequential trapping of zebrafish larvae. The red arrows illustrate the flow velocity fields, and the arrow density indicates the flow rate at specific spots within the dorsal Fish-Trap chips. **(A)** No larva trapped; **(B)** One larva trapped; **(C)** Two larvae trapped; **(D)** Three larvae trapped; **(E)** Four larvae trapped.

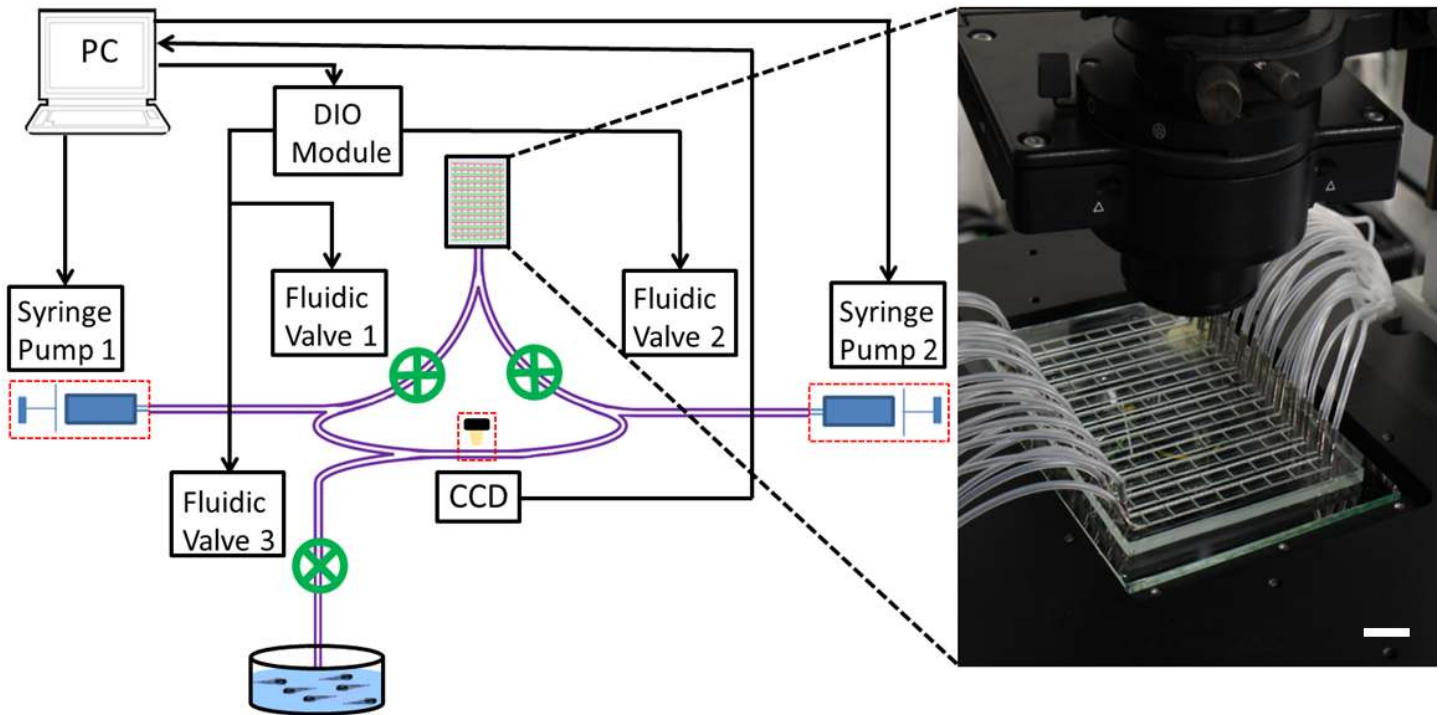


Figure S2. System diagram of different control modules of the Fish-Trap technology, which is an automated system based on a computer-controlled and pump-actuated capillary fluidic circuitry. Scale bar, 2cm.

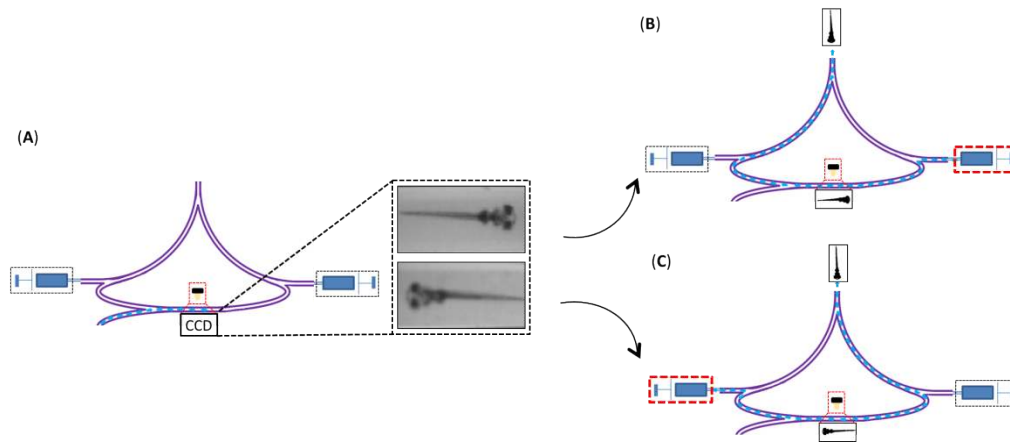


Figure S3. Illustration of the direction-switching-loop. **(A)** Photo-detection system identify the successful loading and the direction of a larva loaded from the reservoir. **(B)** For a larva loaded with head facing forward, the right pump (in red box) is engaged to pump the larva into the Fish-Trap chip. **(C)** For a larva loaded with tail facing forward, the left pump (in red box) is engaged to pump the larva into the Fish-Trap chip. In panel **(B)** & **(C)**, the actually flow direction indicated by the blue dash line.

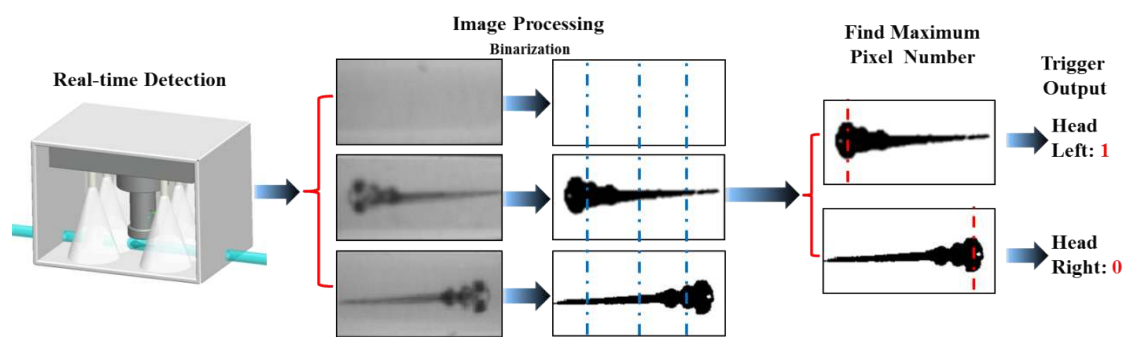


Figure S4. Schematics of the Photo-detection module. The output of this module was used to trigger the valve switching and pump activation.

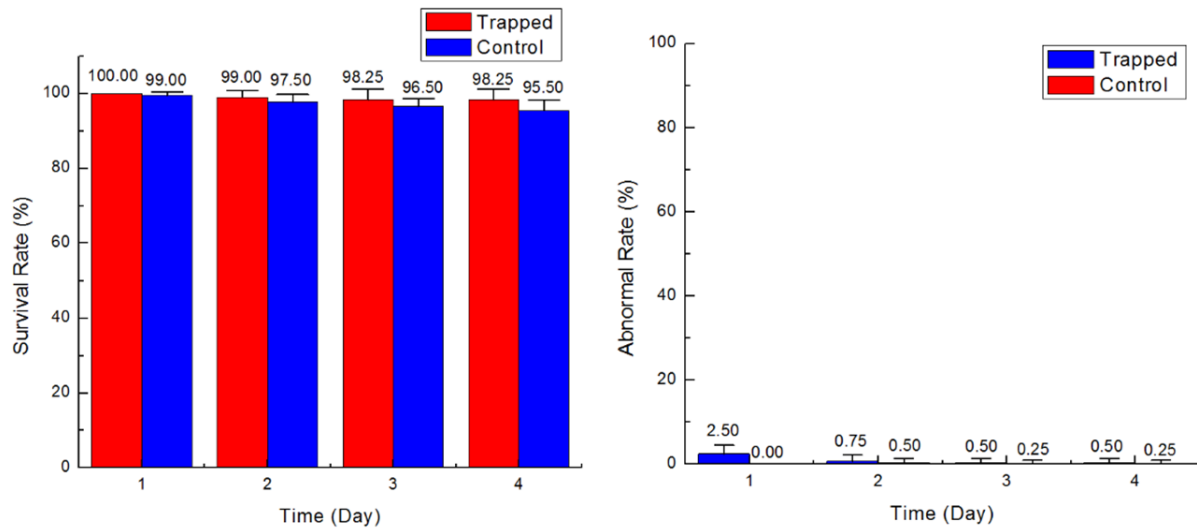


Figure S5. Quantitative health assessment of larvae released from Fish-Trap chips. Survival rate and abnormal rate of zebrafish larvae in the following 4 days after 2 hour trapping in the array. Total 400 larvae pooled from eight independent experiments (50 larvae/experiment) were analyzed. Error bars indicate standard deviation. Our criteria for health assessment include both functional and morphological abnormalities as previously reported (Pardo-Martin *et al* Nat Methods 2010, Chang *et al* Integr Biol 2014). Functional criteria included visual confirmation of normal heartbeat and reflex response to touch stimuli. Morphological criteria included spine bending (i.e. lordosis, kyphosis, and scoliosis) and craniofacial abnormalities.

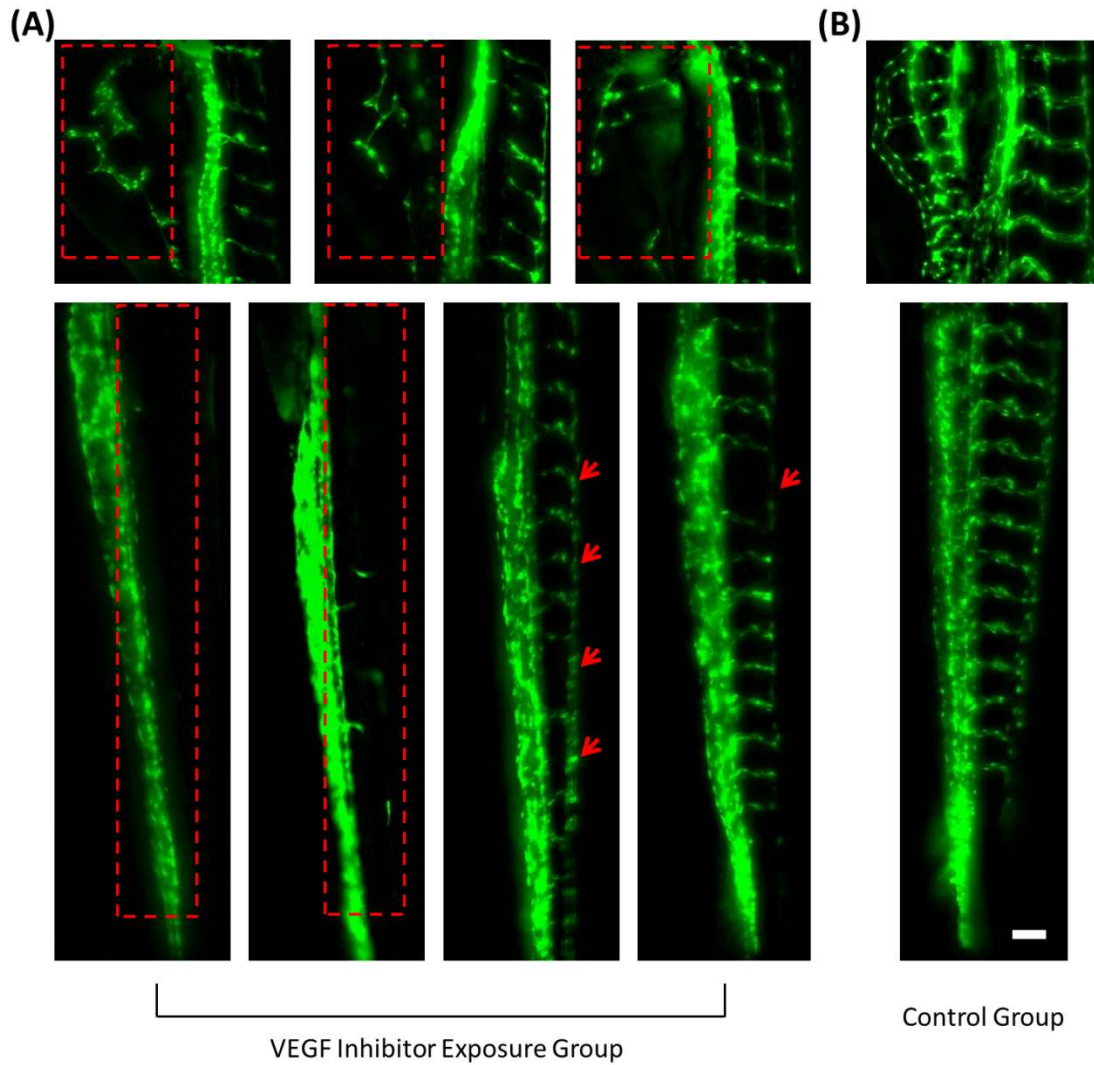


Figure S6. Long term observation of larval zebrafish using lateral Fish-Trap chips. **(A)** Testing group treated with VEGFR inhibitor in larvae from the Fli1 transgenic line. The larvae were on-chip treated with VEGFR inhibitor ($1\mu\text{M}$) for 36 hours, resulting disrupted development of blood vessel development. **(B)** Control group without treatment of VEGFR inhibitor showing normal development of vasculature structures. Scale bar, $50\mu\text{m}$.

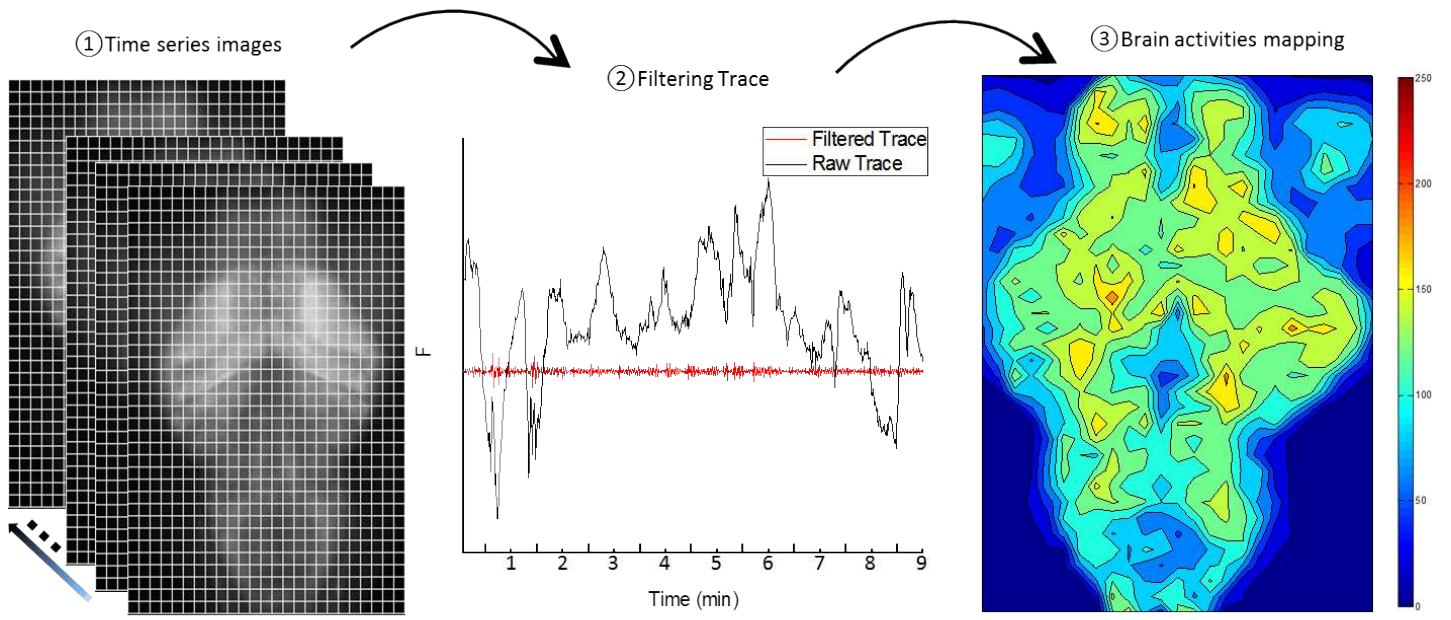


Figure S7. Experimental procedures to derive brain activities density map from calcium imaging data.

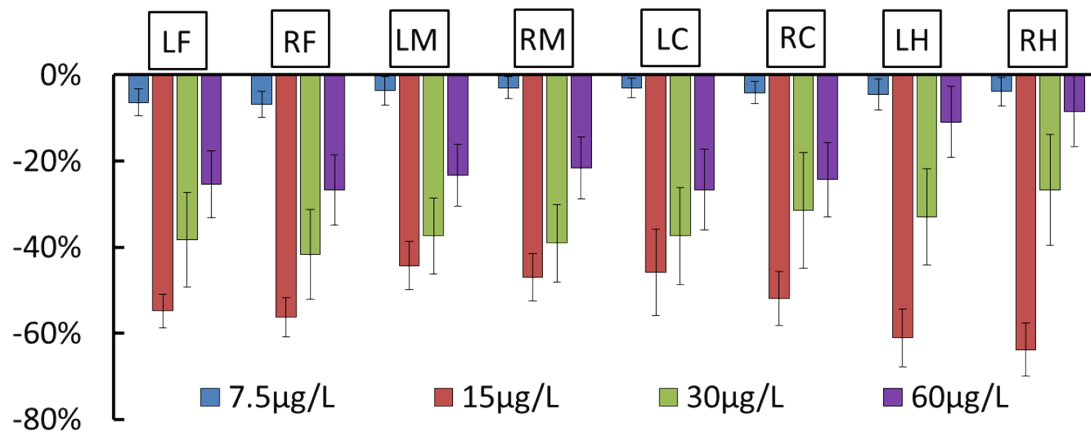



Figure S8. Quantification of dose-response of Con-T[M8Q], showing differential inhibitory effects of neural activity at various concentrations.

Table S1. List of neurotoxins tested in this study.

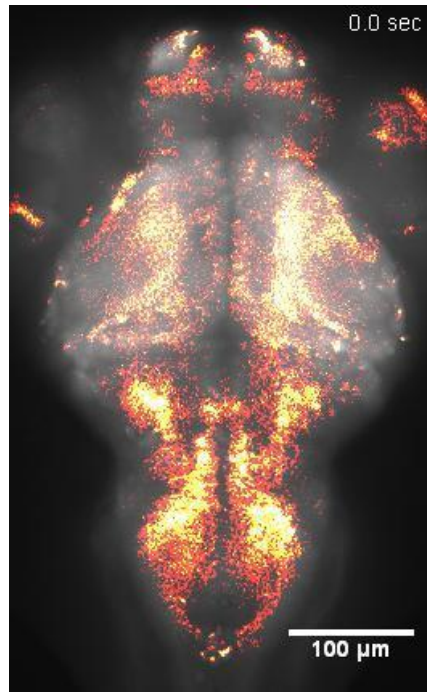
Name	Sequence	Target	References
MVIA	CKGKGAKCSRLMYDCCTGSCRSKGK*	N-type Calcium Channel	1-3
Mr1.8-II	PECCTHPACHVSNPELC*	Unknown	
Mr1.8-I	PECCTHPACHVSNPELC*	nAChR $\alpha 3\beta 2$ subtype	
Vc1.1	GCCSDPRCNYDHPEIC*	nAChR $\alpha 9\alpha 10$ subtype	4, 5
HS-10	Benzoyl-GCCSDPRCRYDHPEIC*	nAChR $\alpha 9\alpha 10$ subtype	
Con-T[M8Q]	GE $\gamma\gamma$ YQKML γ NLR γ AEVKKNA*	NMDAR	6
SO-3	CKAAGKPCSRIAYNCCTGSCRSKGK*	N-type Calcium Channel	7, 8
Nitrendipine	C18H20N2O6	L-type calcium channels	9

1. T. Kohno, J. I. Kim, K. Kobayashi, Y. Kodera, T. Maeda and K. Sato, *Biochemistry*, 1995, **34**, 10256-10265.
2. M. Sanford, *CNS Drugs*, 2013, **27**, 989-1002.
3. M. S. Lee, *Progress in medicinal chemistry*, 2014, **53**, 147-186.
4. R. J. Clark, H. Fischer, S. T. Nevin, D. J. Adams and D. J. Craik, *Journal of Biological Chemistry*, 2006, **281**, 23254-23263.
5. H. Klimis, D. J. Adams, B. Callaghan, S. Nevin, P. F. Alewood, C. W. Vaughan, C. A. Mozar and M. J. Christie, *Pain*, 2011, **152**, 259-266.
6. Z. Sheng, Q. Dai, M. Prorok and F. J. Castellino, *Neuropharmacology*, 2007, **53**, 145-156.
7. Q. Dai, F. Liu, Y. Zhou, B. Lu, F. Yu and P. Huang, *Journal of natural products*, 2003, **66**, 1276-1279.
8. L. Wen, S. Yang, H. Qiao, Z. Liu, W. Zhou, Y. Zhang and P. Huang, *British journal of pharmacology*, 2005, **145**, 728-739.
9. L. D. Hirning, A. P. Fox, E. W. McCleskey, B. M. Olivera, S. A. Thayer, R. J. Miller and R. W. Tsien, *Science*, 1988, **239**, 57-61.

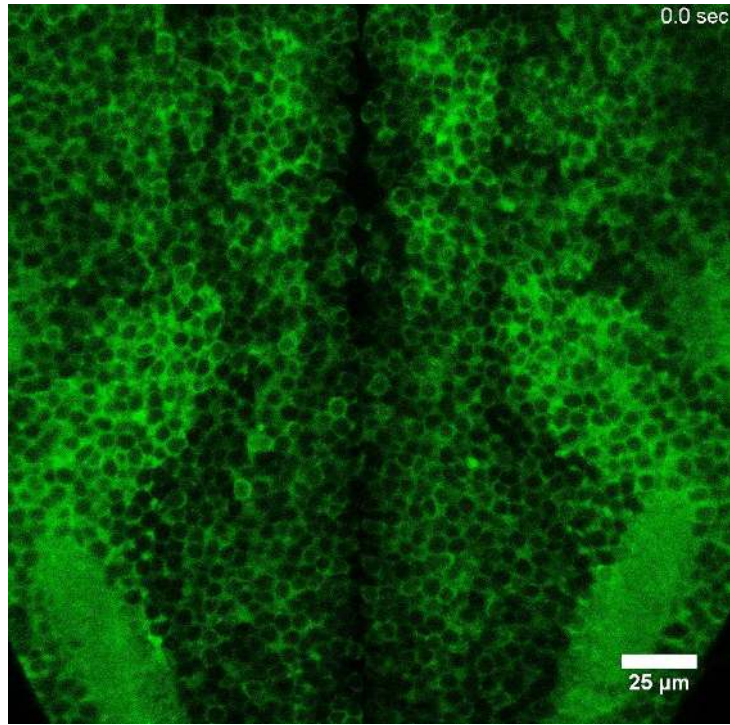


Fish-Trap Technology
Larva loading in dorsal chip

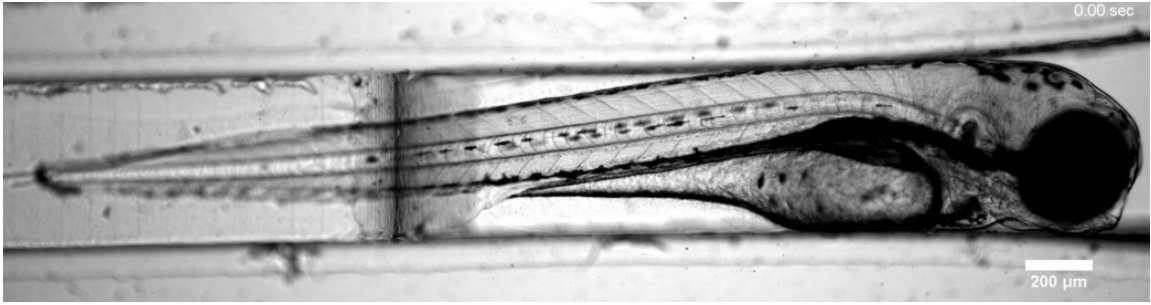
Movie S1. Demonstration of larva loading, trapping and orientation using Fish-Trap technology. Single larva was automatically pushed into the trapping channel by hydrodynamic force.



Movie S2. Real-time mapping of brain-wide activity in brains of larval zebrafish using the Fish-Trap technology.



Movie S3. Calcium imaging with single cell resolution in a brain of fish immobilized using dorsal Fish-Trap chip.



Movie S4. Real-time recording of blood flow in the zebrafish larva immobilized in a lateral Fish-Trap chip.